J Solid State Electrochem (2007) 11:929–938
DOI 10.1007/s10008-007-0285-5

ORIGINAL PAPER

A surface adsorption model for electroless cobalt alloy thin films

Y. Shacham-Diamand · Y. Sverdlov · V. Bogush · R. Ofek-Almog

Received: 4 December 2006 / Revised: 8 January 2007 / Accepted: 5 February 2007 / Published online: 24 April 2007
© Springer-Verlag 2007

Abstract Thin cobalt alloy films have been obtained using electroless deposition solution with two reducing agents: dimethylamine borane (DMAB) and sodium hypophosphite. This system allows spontaneous and self-activated deposition of barrier layers on Cu lines and via contacts for ultra large scale integration (ULSI) interconnects applications. This work presents a study of the solution composition effects on the material properties and composition of the films. First, we present the deposition rates, the electrical resistance, the various element profiles in the thin film, and the thin film roughness. Next, we discuss the film's composition and its dependence on the ratio between the reducing agents composition in the solution. The experimental results suggest that the film phosphorous and boron composition is determined by the surface adsorption rates of the reducing agents. Therefore, a surface co-adsorption model of the two reducing agents is proposed, formulated, analyzed, and compared to the experimental results. Finally, we discuss the model and its significance to the formation of high-quality ultra-thin barrier layers.

Keywords Cobalt · Tungsten · Phosphorous · Boron · Electroless deposition

Dedicated to Professor Dr. Algirdas Vaskelis on the occasion of his 70th birthday.

Y. Shacham-Diamand · Y. Sverdlov · V. Bogush · R. Ofek-Almog
Department of Physical Electronics, School of Electrical Engineering, Faculty of Engineering, Tel-Aviv University, Ramat-Aviv,
Tel Aviv 69978, Israel

Y. Shacham-Diamand (✉)
Department of Applied Chemistry,
School of Science and Engineering, Waseda University,
3-4-1 Okubo, Shinjuku-ku,
Tokyo, Japan
e-mail: yosish@eng.tau.ac.il

V. Bogush
The Research and Development Department of the Belarusian State University of Informatics and Radioelectronics (BSUIR),
Minsk, Belarus

Introduction

Electroless deposition of thin metal films has numerous applications for both functional components (i.e., conductive or magnetic materials) and decorative and protective coatings [1, 14]. Electroless metallization had been widely used for electronics applications, mainly for packaging and printed circuits, and have been recently introduced in micro- and nano-technologies. Electroless deposition of metals offers two major advantages: (a) infinite selectivity and (b) low deposition temperature. Electroless deposition methods are typically with excellent step coverage [2, 3]; however, recent results indicate that super-filling in deep submicron strictures using electroless plating is possible [15].

Cobalt and its alloys may offer high corrosion resistance, unique magnetic, electrical and barrier properties. They are used in aerospace and auto component production, chemical synthesis, and fuel elements, practically in any field with metal coating applications: consumer market, medical, military, and more. Electroless plating is used also in electronics where there is a demand to unique, high-quality thin film structures [4]. Cobalt alloy thin films and structures play a major role in magnetic devices [5] and as protective layers [6] in microelectronics and micro-electromechanical systems. Recent application of ternary cobalt-based layers as diffusion barriers and capping layers for Cu metallization in the ultra large scale integration (ULSI) technology improves

interconnection performance and solves some critical problems such as maintaining low interconnect resistance while preventing contamination by copper [7, 8]. The deposition of cobalt films with low soluble dopants improves barrier properties forming either "stuffed" polycrystalline or amorphous diffusion barrier. In some cases, electroless cobalt alloys form an amorphous phase with embedded nanocrystalline structure [9, 10]. The advantages of electroless CoWP alloys were shown elsewhere, and their deposition mechanisms and properties were discussed [10, 11].

One major problem in cobalt phosphorous alloy deposition is that it requires a special activation step for direct electroless plating on Cu. The commonly used CoWP alloy requires activation by noble metal, typically Pd, activation solution. It was shown that deposition using boron containing reducing agent yield a "Pd-free" self-activation electroless plating [12]. Note that "Pd-free" processes may require also some preliminary surface treatment of the Cu surface before the cobalt electroless plating [12]. The introduction of two reducing agents: (a) hypophosphite as a source for phosphorus and (b) dimethylamine borane as a source for boron realizes the advantages of Pd-free deposition process while adding another parameter for the thin film properties control. Similar to the previously discussed CoWP [9–11] and CoWB [12], CoWPB alloys also demonstrated high stability under thermal treatment in vacuum. Such layers can be used in ULSI, micro electro mechanical systems and other micro-systems technologies as a protective or barrier layers.

This work presents experimental data such as deposition rates, composition, and electrical properties of deposits. The effect of annealing in vacuum on the thin film's characteristics is also presented. The work also presents a co-adsorption model that was devised to explain the relation between the concentrations of the components in the solid to the concentration of their precursors in the liquid.

Experimental

Electroless deposition of CoWPB alloy thin layers was performed on copper surface from sulfate–citrate electroless bath with dimethylamine borane (DMAB) as a primary reducing agent and source for boron. This emulates the application of electroless Co alloy capping layers which is a barrier layer that is deposited on top of the Cu line that are typically produced by the Dual damascene method. Trisodium citrate was used as a complexing agent to form strong cobalt complexes. The working pH value of 9.5–9.7 was adjusted by potassium hydroxide. Sodium hypophosphite was used as second reducing agent and a source for phosphorous. The concentration of NaH_2PO_2 was varied in the range of 0–8.05 g/l to study its effect on the thin film content and properties. The sodium tungstate was employed as a source for tungsten (Table 1). The Na_2WO_4 concentration in the initial solution was kept constant—1 g/l (0.003 M). All chemicals were analytical purity grade. Electroless deposition was performed at 80–85 °C in temperature-controlled cell. Sputtered Cu seed on Ti adhesion layer (~10–20 nm total) on SiO_2/Si system was used as a substrate. Electroless deposition was carried out without Pd-activation. The treatment of the surface in 2–10% DMAB solution serves as an activating step. The CoWPB layer's thickness was varied in the 10–220-nm range. Post-deposition vacuum annealing was performed under residual pressure less than 2×10^{-7} Torr at 400 °C for 1 h.

The thin film thickness, composition, and electrical properties were characterized. The layer thickness was measured using by Tencor "Alpha-step 500" profilometer. The thickness was measured on a step of the deposited layer that was created by selective etching of a small part of the Co alloy in diluted HNO_3 in DI water (1:1). The deposition rate was determined by analyzing the data that were obtained after depositing at various times and measuring the thin

Table 1 Composition and deposition parameters for CoWPB alloy electroless plating solutions

Chemicals	Concentration	
	(M)	(g/l)
Co-sulfate ($CoSO_4{\cdot}7H_2O$)	0.1	28.1
3Na-citrate	0.3	88.23
DMAB	0.069	4
NaH_2PO_2	Variable (0, 0.0094, 0.0189, 0.038, 0.057, 0.069, 0.0759)	Variable (0, 0.5, 1, 2, 4, 6, 7.3, 8.05)
Na_2WO_4	0–0.6	0–20
KOH	to adjust the pH to 9.5–9.6	
HCl	3 ml	
Surfactant RE-610	$1.5.10^{-2}$	
Temperature (°C)	80–85	
pH	9.5–9.7	

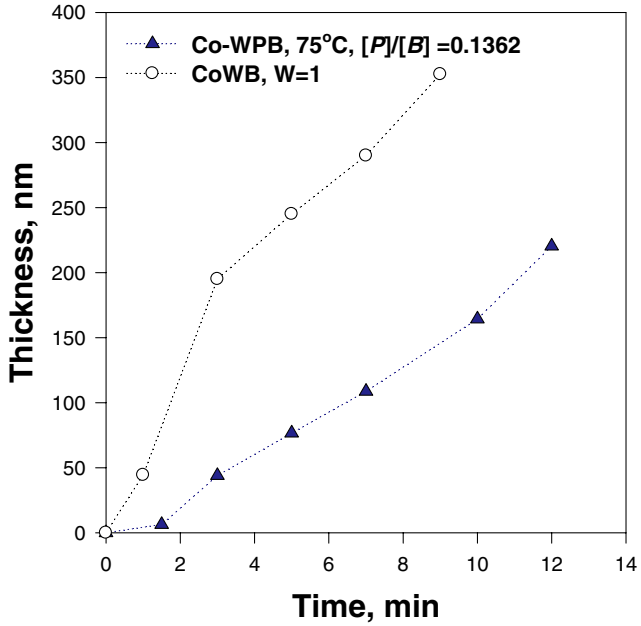

Fig. 1 Thickness of electroless CoWPB films as a function of deposition time, pH=9.5; W-ions concentration is 0.003 M (1 g/l)

film thickness. Thin films composition was analyzed qualitatively and quantitatively by secondary ion-mass spectroscopy (Perkin Elmer TOF-SIMS). The SIMS experimental conditions were: (a) profiling using a 15 keV Ga^{+} 2 nA analytical gun and (b) sputtering using a 2-kV O^{2+} sputter gun. Under the given sputtering and data sampling rates, the estimated relative error in the SIMS signals as calculated from the deviation from the average over the thin layer thickness was approximately 5%. The sheet resistance and resistivity of the films were measured by in-line four-point probe made by Lucas/Signatone™. Roughness and top views were analyzed by atomic force microscope (AFM) model Nanoscope IV, and SEM images were taken by a cold field emitter high resolution SEM model JEOL 6700F.

Results

Electroless deposited CoWPB thin films demonstrated high adhesion to the substrate, uniformity over sample surface, good coverage. The deposition reaction has autocatalytic nature, and layer thickness is controlled by deposition time and reagent concentration in solution.

Deposition rate

The deposition rate was ~40 nm/min for solution with DMAB only, and it dropped to the 15 to 20-nm/min range when the hypophosphite ion was added (Fig. 1). Increasing the concentration of the hypophosphite ion did not change much the deposition rate that reached a maximum of ~25 nm/min when the hypophosphite ions reached their maximum value according to Table 1.

Resistivity

The CoWPB thin films sheet resistance (Rs) measurements are shown in Fig. 2a. The cobalt alloy was deposited on a very thin (~5 nm) Cu underlayer that was deposited on a thin (5 nm) titanium adhesion layer. As the data included also the influence of the copper under-layer, we extracted the true Co alloy sheet resistance by plotting 1/Rs vs the thin film thickness (d), and assuming two resistors in parallel model:

$$1/\mathrm{Rs} = 1/\mathrm{Rs}(\text{Cu underlayer}) + d/\rho \quad (1)$$

Where ρ is the resistivity of the Co alloy thin film. Such analysis is shown in Fig. 2b. First, we calculate the effective under-layer sheet resistance; next, we extract the Co alloy resistivity from the slope of the curve (Fig. 3).

The calculated resistivity of CoWPB layer was in the order of 5×10^{-5} Ω cm. This value was almost similar for

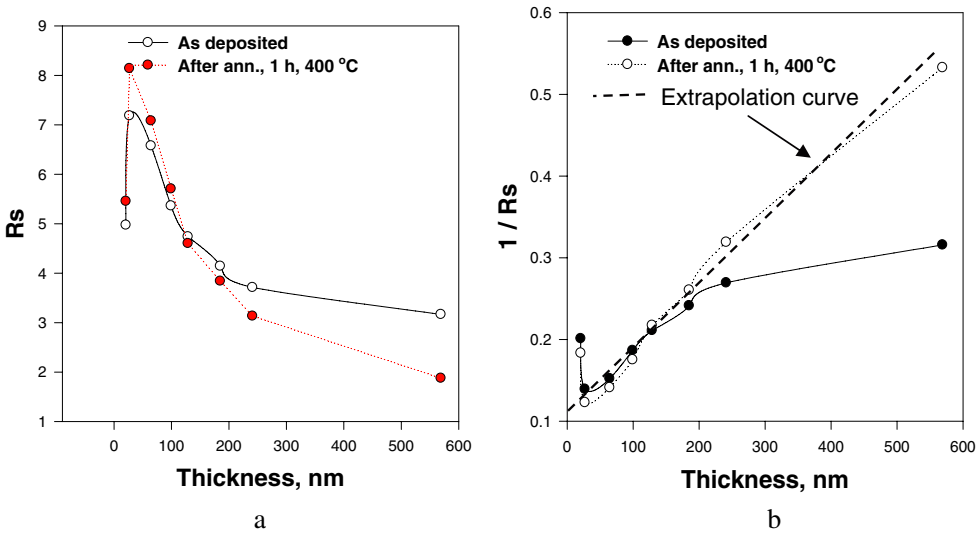

Fig. 2 **a** Sheet resistance (*Rs*) of electroless CoWPB films as a function of film thickness in as-deposited and annealed state. **b** 1/Rs vs thickness

most of the samples and did not change significantly after vacuum treatment at 400 °C for 1 h.

Composition of deposited films

Typical results of SIMS profiling of thin films with different solutions are shown in Figs. 4 and 5. Most of the results indicated that the film composition was uniform as a function of depth. However, the solution with the lowest concentration of hypophosphite yielded thin films with non-uniform composition. This may be explained by the effect of initial reaction stage, when reducing process is realized predominantly by dimethylamine borane. Therefore, we excluded this data from the following analysis. Increasing the NaH_2PO_2 concentration above 2 g/l ($[H_2PO_2^-]/[DMAB]$= 0.8) caused the level of tungsten and boron concentration in the deposits to decrease to such level where it was comparable to the measurement instrument noise level. It was found, by X-ray photoelectron spectroscopy (XPS) analysis, that the tungsten is included mainly in an oxidized form (WO_2). It was also observed that the phosphorous forms a noticeable compound with cobalt.

A summary of the Co alloy composition, using the solutions that are described in Table 1, is given in Fig. 6. In this case, we preferred to plot the various composition vs the ratio between the hypophosphite ion and the DMAB. The reason for that plot will be explained in the coming section where we present the deposition adsorption limited model.

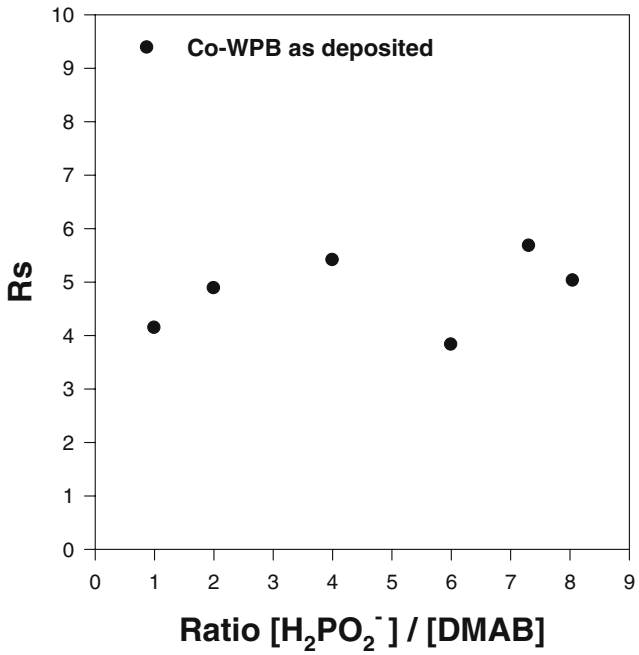

Fig. 3 Sheet resistance of electroless CoWPB films as a function of reducing agents ratio $[H_2PO_2]/[DMAB]$ in solution. Time of deposition is 10 min

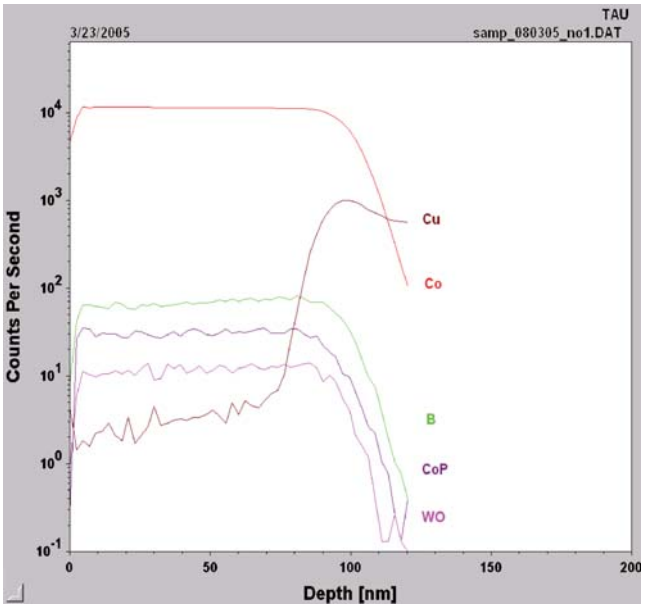

Fig. 4 SIMS profile of chemical deposited CoWPB film from electrolyte with NaH_2PO_2 concentration of 1 g/l (0.0094 M)

SEM and AFM measurements

Roughness measurements were carried out for CoWPB thin films obtained from electrolyte with NaH_2PO_2 and DMAB concentrations of 1 and 4 g/l, correspondingly. Results of those measurements are given in Table 2 and Fig. 7. We present roughness for layers with thickness 150 and 570 nm. Those are relatively thick layers, much thicker than what is required for capping layers (in the range of 10–

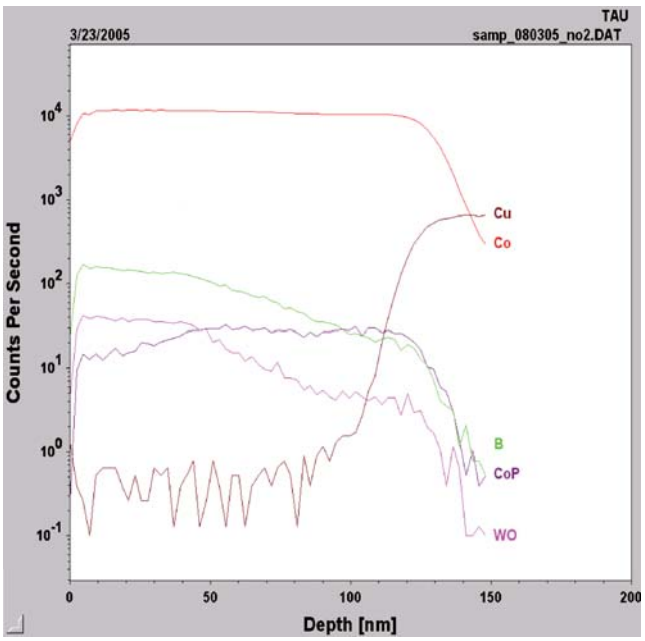

Fig. 5 SIMS profile of electroless CoWPB film. The deposition was performed from solution with concentration of tungsten 1 g/l (0.003 M) and sodium hypophosphite 0.5 g/l (0.0047 M)

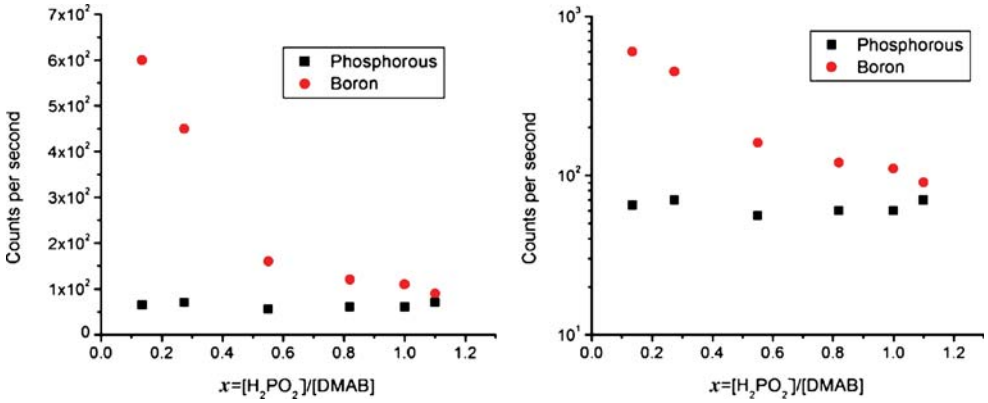

Fig. 6 The SIMS signal, in counts per second, for the boron and phosphorous in the thin film (*Left* linear scale; *right* log–lin scale) as a function of the ratio between the hypophosphite ions to the DMAB concentration (see Table 1). The DMAB concentration was kept at 4 g/l

20 nm or less). The results indicated on very low relative roughness in the range of 1% of the film thickness. We can see from Table 2 that the roughness of the deposited films increases with increasing of the thickness.

SEM images are shown in Fig. 8 for layers with thickness $t_f \sim 10$ nm and $t_f \sim 150$ nm. The results show significant morphology change after annealing at 400 °C.

Discussion

A major clue towards a model of the deposition of Co alloy was discovered when we plot the inverse of the boron concentration vs the hypophosphite to DMAB concentration ratio (Fig. 9). This transformation yields a straight line that indicates on an empirical model:

$$\frac{1}{[B]_{film}} = \frac{1}{[B]_{film,0}} + Const. \cdot \frac{[H_2PO_2^-]}{[DMAB]} \quad (2)$$

To acquire a better understanding of the micro-mechanism in a solution with two reducing agents, a co-deposition model was developed. We assume that the mathematical dependence between the ratio of the two reducing agents and the concentration in the solid film indicates that the composition is determined by some surface reaction that is determined by that ratio. This is based on the fact that the main reducing agent is the source of boron in the complex DMAB, and the second reducing agent, the ion $H_2PO_2^-$ (from the sodium hypophosphite, NaH_2PO_2), is the source of phosphorous.

The model is based on the work of T. Homma and T. Shimada from Waseda University, Tokyo, Japan using molecular orbital (MO) calculations (T. Homma, T. Shimada, private communication, Waseda University, Tokyo, Japan). They used this calculation method to estimate the co-adsorption energies of the two reducing agents.

In the next few sections, we will build a model that predicts the concentration of boron and phosphorous in the solid versus the solution concentration of the various components. We will outline a surface adsorption-limited model that describes the situation in the case of both phosphorous and boron containing reducing agents. We do not take into consideration the interaction between the two reducing agents and also neglect the effect of the tungsten.

Co-adsorption deposition model

In this section, we will describe simple model that predicts the concentration of phosphorous and boron in the solid as a function of the DMAB and hypophosphite concentration in the liquid. We assume constant temperature and pH in all the samples. Also, all other component concentration remains the same in all the experiments.

In this, we assume a simple first-order adsorption model without interaction.

The co-adsorption coefficients can be given as:

For DMAB:

$$A_B = k_B \cdot [DMAB] \cdot e^{-\frac{\Delta G_B}{RT}} \quad (3)$$

For $H_2PO_2^-$:

$$A_P = k_P \cdot \left[H_2PO_2^-\right] \cdot e^{-\frac{\Delta G_P}{RT}} \quad (4)$$

Where ΔG_B and ΔG_P are the co-adsorption free energies and k_B and k_P are constants.

Table 2 Roughness of electroless deposited CoWPB films determined by AFM measurement

CoWPB thin film	R_{ms} (R_q) (nm)	Mean roughness R_a (nm)	Max height, R_{max} (nm)
[P]=1 g/l, as dep. 150 nm	1.925	1.596	9.223
[P]=1 g/l, 150 nm, 2 h at 400 °C	1.605	1.256	8.605
[P]=1 g/l, as dep. 570 nm	5.442	4.258	34.968
[P]=1 g/l, 570 nm 2 h at 400 °C	6.293	5.129	37.558

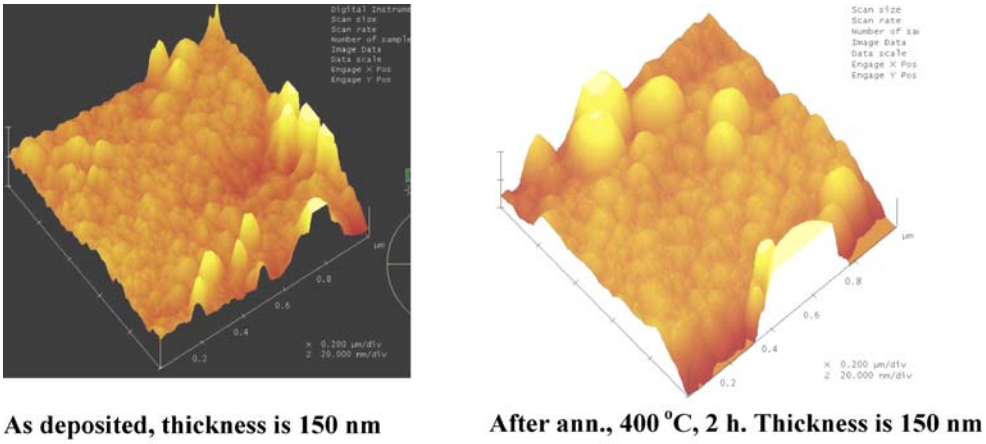

Fig. 7 AFM top view of chemical deposited CoWBP thin films

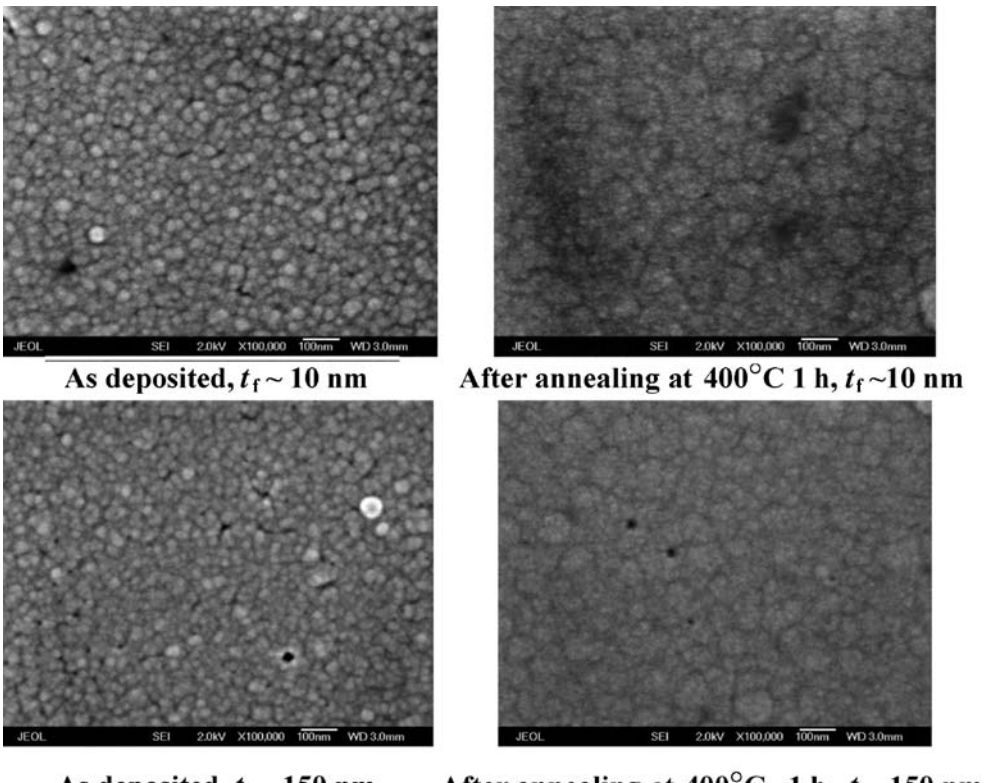

Fig. 8 SEM images of electroless deposited CoWPB films on thin Cu seed layer

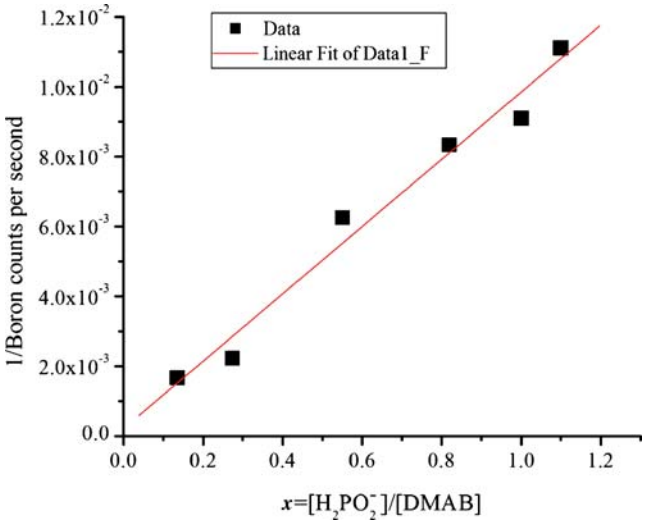

Fig. 9 One over the boron SIMS signal as a function of the hypophosphite to DMAB ratio

First, we present a short review of the deposition model of each one of the reducing agents. In the case where the reduction agents are based on the hypophosphite ($H_2PO_2^-$) ions, we can assume a general model as it appears in [1]:

$$Co^{2+} + H_2PO_2^- + H_2O \rightarrow Co^0 + H_2PO_3^- + 2H^+ \quad (5a)$$

$$H_2PO_2^- + H_2O \xrightarrow{cat} H_2PO_3^- + H_2 \quad (5b)$$

A few models of phosphorous deposition were mentioned in the literature:

Reaction with adsorbed hydrogen [16, 17]

$$H_2PO_2^- + H \rightarrow P + H_2O + OH^- \quad (6)$$

Hydride transfer mechanism [18],

Electrochemical model [19],

$$H_2PO_2^- + 2H^+ + e \rightarrow P + 2H_2O \quad (E^0 = 0.501\ V) \quad (7)$$

Coordination of hydroxyl ions and hexaquonickel ion [20].

All the models assume that the concentration of phosphorous in the solid film is proportional to the concentration of adsorbed $H_2PO_2^-$. Therefore, we define a proportional constant η_P, so that

$$[P]_{film} = \eta_P \cdot \left[H_2PO_2^-\right]_{adsorbed} \quad (8)$$

In the case of the boron deposition process by the reducing agent DMAB, the reaction is assumed to be as follows [16]:

$$R_2NHBH_3 \rightarrow R_2NH + BH_3 + H_2 + H^+ \rightarrow R_2NH^+ + B + 5/2\ H_2 \quad (9)$$

Similar to the case with the phosphorous, we also assume that the concentration of boron in the solid film is proportional to the concentration of adsorbed DMAB. The proportion constant is defined as η_b,:

$$[B]_{film} = \eta_B \cdot [DMAB]_{adsorbed} \quad (10)$$

The coefficients η_B and η_P might also be a function of the concentration of the species in the solution. However, we assume that even if they vary, the function is a weak one and does not affect much the model that is proposed here. In addition, there can be other effects such as cross-interaction between the two reducing agents that we neglect in the model presented here.

Next, we define the rate equations for the adsorption sites:

$$\frac{dN_B}{dt} = A_B \cdot (N_0 - N_P + N_B) - \frac{N_B}{\tau_B} \quad (11)$$

$$\frac{dN_P}{dt} = A_P \cdot (N_0 - N_P + N_B) - \frac{N_P}{\tau_P} \quad (12)$$

Where:

- N_0 the number of the total available sites for adsorption on the surface (cm^{-2})
- N_B the number of sites where the DMAB has been adsorbed (cm^{-2})
- N_P the number of sites where the $H_2PO_2^-$ has been adsorbed (cm^{-2})
- A_B DMAB adsorption coefficient
- A_P H_2PO_2-adsorption coefficient
- τ_B mean time to disappearance of the sites with adsorbed DMAB
- τ_P mean time to disappearance of the sites with adsorbed $H_2PO_2^-$

In addition, we assume that the total deposition rate, R, is the sum of the deposition rate due to DMAB reduction, R_B, and the deposition rate due to reduction by the $H_2PO_2^-$ ion, R_P. We neglect cross-reduction effects where one reducing agent may affect the reducing capabilities of the second ion due to some chemical proximity effect.

The DMAB- and $H_2PO_2^-$- induced deposition rates are determined by the following relations:

$$R_B = \Omega\, N_B/\tau_B, \quad (13a)$$

$$R_P = \Omega\, N_P/\tau_P. \quad (13b)$$

Where Ω is the thin film atomic volume. We assume that the reduction reaction is complete in the sense that every single reduction reaction creates one cobalt ion being deposited. Additionally, we assume that the deposition rate

is determined by the adsorption rates. Therefore, $1/\tau_B$, $1/\tau_P >> A_P, A_B$.

In the case of steady state where both rate equations are equal to zero, we obtain the following relations:

$$N_B/\tau_B = A_B\, N_0\ , \tag{14a}$$

$$N_p/\tau_p = A_p\, N_0\ . \tag{14b}$$

Therefore, the total deposition rate R is given by:

$$R = \Omega\, N_0(A_P + A_B) \tag{15}$$

While the deposition rate due to each of the reducing agents is given by:

$$R_B = \Omega\, N_0\, A_B, \tag{16a}$$

$$R_P = \Omega\, N_0\, A_P. \tag{16b}$$

The concentration of the boron and the phosphorous in the solid depends on the ratio between the fractional deposition rate to the total rate:

$$[B]_{film} = \frac{\eta_B \cdot R_B}{R} = \frac{\eta_B \cdot A_B}{A_B + A_P} \tag{17a}$$

$$[P]_{film} = \frac{\eta_P \cdot R_P}{R} = \frac{\eta_P \cdot A_P}{A_P + A_P} \tag{17b}$$

Where η_P and η_B are fitting parameters; the total deposition rate R is the sum of the partial deposition rates, R_B and R_P.

Given this basic relations, we can now calculate the boron and phosphorous concentration in the sold as a fiction of the solution composition.

Boron concentration

When we substitute the expressions of the adsorption coefficients (Eq. 3 and 4) in Eq. 17a and b, we receive the following expression for the concentration of the boron in the film:

$$[B]_{film} = \frac{\eta_B \cdot k_B \cdot [DMAB] \cdot e^{-\frac{\Delta G_B}{RT}}}{k_B \cdot [DMAB] \cdot e^{-\frac{\Delta G_B}{RT}} + k_P \cdot \left[H_2 PO_2^-\right] \cdot e^{-\frac{\Delta G_P}{RT}}} \tag{18}$$

The terms in this expression can be reorganized to a form which is similar to the experimentally found expression 2:

$$\frac{[B]_{film}}{[B]_{film,0}} = \frac{1}{1 + \frac{k_P}{k_B} \cdot \frac{\left[H_2PO_2^-\right]}{[DMAB]} \cdot e^{\frac{\Delta G_B - \Delta G_P}{RT}}} \tag{19}$$

The theoretical calculations using the MO model [16] show that the Gibbs free energy of the reduction reaction by the hypophosphite is less than that by DMAB, i.e., $\Delta G_P < \Delta G_B$. This result was found both on Co and on Cu substrates. Therefore, as the reduction by the $H_2PO_2^-$ is favorable compared to the reduction by the DMAB, we may assume that:

$$\frac{\eta_P \cdot k_P}{\eta_B \cdot k_B} \cdot \frac{\left[H_2PO_2^-\right]}{[DMAB]} \cdot e^{\frac{\Delta G_B - \Delta G_P}{RT}} > 1 \tag{20}$$

We define:

$$k_{B1} = \frac{k_P}{k_B} \cdot e^{\frac{\Delta G_B - \Delta G_P}{RT}} \tag{21}$$

Finally, the concentration of the boron in the film can be written as follows:

$$[B]_{Film} = \frac{[B]_{Film,0}}{1 + k_{B1} \cdot \frac{\left[H_2PO_2^-\right]}{[DMAB]}} \tag{22a}$$

Or in a slightly different form, that shows a linear relation as shown in Fig. 8:

$$\frac{[B]_{Film,0}}{[B]_{Film}} = 1 + k_{B1} \cdot \frac{\left[H_2PO_2^-\right]}{[DMAB]} \tag{22b}$$

This theoretical result seems to yield a similar function to that of what we found experimentally.

Phosphorous concentration

A similar calculation can be made for phosphorous:

$$[P]_{film} = \frac{\eta_P \cdot k_P \cdot \left[H_2PO_2^-\right] \cdot e^{-\frac{\Delta G_P}{RT}}}{k_B \cdot [DMAB] \cdot e^{-\frac{\Delta G_B}{RT}} + k_P \cdot \left[H_2PO_2^-\right] \cdot e^{-\frac{\Delta G_P}{RT}}} \tag{23}$$

Or:

$$\frac{[P]_{film}}{[P]_{film,0}} = \frac{1}{1 + \frac{k_B}{k_P} \cdot e^{\frac{\Delta G_P - \Delta G_B}{RT}} \cdot \frac{[DMAB]}{\left[H_2PO_2^-\right]}} \tag{24}$$

We can rewrite this equation as:

$$\frac{[P]_{film}}{[P]_{film,0}} = \frac{1}{1 + \frac{1}{x}} = \frac{x}{x+1} = \frac{k_{B1} \cdot \frac{\left[H_2PO_2^-\right]}{[DMAB]}}{k_{B\,1} \cdot \frac{\left[H_2PO_2^-\right]}{[DMAB]} + 1} \tag{25}$$

Where we define

$$x \equiv k_{B1} \cdot \frac{\left[H_2PO_2^-\right]}{[DMAB]} \tag{26}$$

Those results show that the phosphorous concentration should reach an almost constant value as the hypophosphite ions concentration increases.

The experiment that is shown in Fig. 6 shows that the phosphorous concentration in the solid increased rapidly as hypophosphite ions were added and reached an almost constant value for $\left[H_2PO_2^-\right]/[\mathrm{DMAB}] > 0.136$. The SIMS signal in the range of $0.136 < \left[H_2PO_2^-\right]/[\mathrm{DMAB}] < 1.1$ was about 60 to 70 counts per second on average for all the samples, with an estimated peak to peak noise of about 10 counts per second. This value yielded a phosphorous concentration that was estimated by the SIMS calibration data to be in the range of 4–6%. XPS data yielded a lower phosphorous concentration of ~2.5–3%, with a value that was also almost a constant for the various $x = \left[H_2PO_2^-\right]/[\mathrm{DMAB}]$ ratios. Those results, both for the phosphorous and the boron concentration in the solid, comply with the model that is proposed in this paper.

Summary and conclusions

The paper presents both the results and the modeling of thin cobalt alloy films that have been deposited by electroless plating. We present a system with mixed two reducing agents and the effect of solution composition on structure and electrical properties of deposits. Mixing both sodium hypophosphite and dimethylamine borane reducing agent with cobalt metal ionic solution and tungstate ions at a lightly basic solution (pH~9.5) yielded a self-activated spontaneous deposition of cobalt–tungsten–phosphorous–boron (CoWPB) thin-film coatings formation. Adding hypophosphite to solution with DMAB only reduced the deposition rate from ~40 nm/min to about 20 nm/min at 90 °C. The solution composition was studied intensively, and the functional dependence between the solid to the liquid composition pointed towards an adsorption limited model. Such model was developed and showed that it can be used to explain the experimental results.

Prediction of the electroless plating composition is of prime importance. Each component has a specific role in the thin film properties. For example, it is assumed that adding tungsten, boron, and phosphorous improves the film barrier properties against copper diffusion. However, the relative role of each component may differ. It is also known that adding tungsten affects oxidation resistance of Co, most likely due to the formation of tungsten-oxide that applies mechanical stress on the grain boundaries that allows oxygen penetration and faster grain boundary oxygen diffusion and cobalt oxidation. Therefore, to balance between the need for a good barrier and good corrosion resistance, some tungsten is added to the film, but not too much. Therefore, a good composition model is required to allow thin film development process and a reproducible process control.

The co-adsorption model that is described here is a simple one and should be further developed. It is only at its beginning stage and definitely requires refinement. However, early results show that this model is in agreement with the experimental data regarding the concentration of boron and phosphorous in Co alloy deposited by the electroless method. In the model that is described in this paper, we did not take into consideration cross-adsorption effects, i.e., the effect of one species on the adsorption processes of other species. We also neglected the effect of the tungstate ions. A study on the effect of the tungstate ion in the solution on the co-adsorption model is under way and will be published in the near future.

Finally, note that although we present data and discuss a deposition process with tungsten as the refractory metal, other refractory metals are also possible, such as molybdenum [14] or rhenium [5] to form thin barrier layers for ULSI metallization. However, it is not clear yet whether the model that is presented in this paper is valid for the electroless plating of cobalt alloys with other refractory metals.

Acknowledgments The authors would like to thank Dr. Larisa Burschstein and Dr. Alexander Gladkikh from the Wolfson Material Research Center at Tel-Aviv University. We also want to thank Prof. T. Homma and Mr. T. Shimada from Waseda University, Tokyo, Japan for letting us use the results of their molecular orbital (MO) calculations. Finally, cordial thanks for Prof. T. Osaka and Dr. M. Yoshino from Waseda University for many useful discussions regarding electroless cobalt and nickel alloy deposition.

This work was partly supported by a Grant-in-Aid from the Ministry of Education, Culture, Sports, Science and Technology, Japan for: (a) the Center of Excellence (COE) Research "Establishment of Molecular Nano-Engineering", (b) the 21st Century COE Program "Practical Nano-Chemistry", and (c) the consolidated Research Institute for Advanced Science and Medical Care (ASMeW)

References

1. Mallory GO, Hajdu JB (eds) (1990) Electroless plating: fundamentals and applications. William Andrew Publishing, Norwich
2. Datta M, Osaka T, Schultze JW (eds) (2005) Microelectronic packaging. New trends in electrochemical technology, vol 3. CRC, New York, pp 111–148
3. Shacham-Diamand Y, Dubin VM, Angyal M (1995) Thin Solid Films 262:93
4. Dubin VM (2003) Microelectron Eng 70:461
5. Osaka T, Kasai N (1981) J Met Finish Soc Jpn:309
6. Kohn A, Eizenberg M, Shacham-Diamand Y (2002) J Appl Phys 92:5508

7. Shacham-Diamand Y (2001) J Electron Mater 30:336
8. Shacham-Diamand Y, Lopatin S (1999) Electrochim Acta 44:3639
9. Kohn A, Eizenberg M, Shacham-Diamand Y (2003) Appl Surf Sci 212–213:367
10. Kohn A, Eizenberg M, Shacham-Diamand Y (2003) J Appl Phys 94:3810
11. Petrov N, Sverdlov Y, Shacham-Diamand Y (2002) J Electrochem Soc 149:C187
12. Bogush V, Sverdlov Y, Einati H, Shacham-Diamand Y (2004) Proceedings of the Advanced Metallization Conference 2004 (AMC 2004). MRS Publications, San Diego
13. Shacham-Diamand Y, Zylberman A, Petrov N, Sverdlov Y (2002) Microelectron Eng 64:315
14. Gorbunova KM (ed) (1974) Physico-chemical origins of the chemical reduction of cobalt. Science Publishing, Moscow (in Russian)
15. Hasegawa M, Okinaka Y, Shacham-Diamand Y, Osaka T (2006) Electrochem Solid State Lett 9:C138
16. Gutzeit G (1959) Plating 46:1158
17. Gutzeit G (1960) Plating 47:63
18. Brenner A, Riddell GE (1946) J Res Natl Bur Stand 37:31
19. Brenner A, Riddel GE (1947) J Res Natl Bur Stand 39:385
20. Salvago G, Cavallotti PL (1972) Plating 59:665